

Original Research

The Role of NF- κ B/MIR155HG in Regulating the Stemness and Radioresistance in Breast Cancer Stem Cells

Yunbao Xu^{1,*}, Lu Yang¹, Guangming Li², Chuangzhou Rao¹

Academic Editor: Alfredo Budillon

Submitted: 23 July 2024 Revised: 28 October 2024 Accepted: 4 November 2024 Published: 20 January 2025

Abstract

Background: Breast cancer stem cells (BCSCs) are instrumental in treatment resistance, recurrence, and metastasis. The development of breast cancer and radiation sensitivity is intimately pertinent to long non-coding RNA (lncRNA). This work is formulated to investigate how the lncRNA MIR155HG affects the stemness and radioresistance of BCSCs. **Methods**: Effects of MIR155HG knockdown on BCSCs were gauged in MCF-7 and MDA-MB-231 cell lines. MIR155HG expression was manipulated in cells, followed by an assessment of stemness, DNA damage repair, apoptosis, cell cycle, and the Wnt signaling pathway under radiation conditions. The interaction between nuclear factor kappa B (NF-κB) subunit RelA and MIR155HG was examined using a dual-luciferase reporter assay. To examine the binding interaction between RelA and MIR155HG promoter, chromatin immunoprecipitation was performed. **Results**: Breast cancer-derived stem cells exhibited a high level of MIR155HG. Knockdown of MIR155HG reduced stemness, enhanced radiosensitivity, induced apoptosis, and arrested cells in the G1 phase. Mechanistically, MIR155HG knockdown repressed Wnt/β -catenin signaling and mediated apoptosis-related protein expressions. NF-κB subunit RelA transcriptionally activated MIR155HG, thereby contributing to radioresistance in BCSCs. **Conclusion**: NF-κB regulates MIR155HG transcriptionally to activate the Wnt pathway, thus enhancing stemness and radioresistance in BCSCs. Targeting MIR155HG may enhance the susceptibility of cancer stem cells to radiation-induced cell death, potentially improving therapeutic outcomes. These findings underscore MIR155HG as a promising therapeutic target for breast cancer.

Keywords: breast cancer; cancer stem cells; nuclear factor-kappa B; MIR155 host gene

1. Introduction

Breast cancer is a highly prevalent malignant tumor arising from breast tissue in women globally. According to statistics from the World Health Organization, breast cancer ranks first among malignant tumors in women, with new cases of roughly 2.3 million and deaths of around 685,000 annually [1]. Breast cancer has a complicated etiology that involves genetics, hormone levels, lifestyle, and environmental exposures [2]. Various treatment modalities exist, such as radiation, endocrine therapy, chemotherapy, surgery, and targeted therapy [3], of which radiotherapy is instrumental in controlling local tumor and reducing recurrence rates. However, radiotherapy has been confirmed to stimulate tumor stem cells to secrete cytokines or enhance DNA damage repair mechanisms, leading to increased selfrenewal capacity and radioresistance [4]. Furthermore, tumor stem cells extracted from glioblastoma xenografts and live tissues are associated with radioresistance and tumor cell regeneration [5]. Stem cells from breast cancer display significantly higher invasion ability, proliferation capacity, and radioresistance compared to non-stem cells [6]. The presence of breast cancer stem cells (BCSCs) provides a possible explanation for the current treatment resistance, recurrence, and metastasis, indicating that inhibiting these stem cells-related signaling pathways could be promising in reversing chemoradiotherapy resistance.

Long non-coding RNA MIR155 host gene (lncRNA MIR155HG) is located on chromosome 21 of the human genome [7]. MIR155HG is transcribed into precursor miRNA, which is subsequently processed into mature miR-155. Numerous biological systems, including the immune system, inflammatory reactions, cell proliferation, and differentiation, depend on MIR155HG [8,9]. Morman[10] showed that an early and persistent event in T cell activation is the transcriptional activation of MIR155HG. MIR155HG expression is abundant in various cancers, such as natural killer/T-cell lymphoma [11], cervical cancer [12] and melanoma [13]. In Hodgkin's lymphoma, aberrant B-cell receptors may generate MIR155HG [14]. Under specific conditions, MIR155HG can be processed to produce miR-155, accelerating the progression of glioma [15]. According to earlier research, the MIR155HG/miR-155 axis promotes the epithelial-mesenchymal transition, which is thought to have carcinogenic properties in gliomas [16]. By sponging miR-185, overexpressed MIR155HG in glioblastoma can increase ANXA2 expression, and ANXA2 subsequently binds to the phosphorylated STAT3 and the MIR155HG promoter for stimulating MIR155HG expression and promoting tumor growth and development [17].

¹Department of Chemoradiotherapy, Ningbo No 2 Hospital, 315000 Ningbo, Zhejiang, China

²Department of Breast Surgery, Ningbo No 2 Hospital, 315000 Ningbo, Zhejiang, China

^{*}Correspondence: xyyu20056@sohu.com (Yunbao Xu)

Additionally, it has been proved that *MIR155HG* activates the Wnt signaling pathway to enhance cell radioresistance [18,19]. However, its functional role in regulating BCSCs and radiosensitivity has not yet been documented.

We discovered that BCSCs have high expression of lncRNA MIR155HG through experimental investigation and bioinformatics analysis. Our findings suggested that nuclear factor kappa B (NF- κ B) stimulates the transcription of MIR155HG, which in turn increases BCSCs stemness and radioresistance by promoting Wnt signaling pathway activation. This discovery not only reveals the vital role of MIR155HG in BCSCs but greatly theoretically supports new therapeutic strategies development, contributing to breast cancer patients' prognosis and treatment outcomes.

2. Methods and Materials

2.1 Cell Culture

AnWei-sci (Shanghai, China) provided human breast cancer cell lines MCF-7 (AW-CELLS-H0213) and MDA-MB-231 (AW-CELLS-H0217). Short tandem repeat (STR) analysis was leveraged to validate the purity and ensure cell line stability. All cells underwent mycoplasma testing and were mycoplasma free. Cells were cultured in Dulbecco's Modified Eagle Medium (C0891-100 mL) supplemented with 10% fetal bovine serum (C0251), 100 μg/mL streptomycin (C0222), and 100 U/mL penicillin. All reagents were provided by Beyotime (Shanghai, China).

2.2 Cancer Stem-like Cell Sorting

MCF-7 and MDA-MB-231 cells were initially sorted for CD44⁺ cells using magnetic cell sorting (MACS; Miltenyi Biotech, Auburn, CA, USA) before executing the side population (SP) sorting in order to separate CD44⁺/CD24⁻ cell populations [20]. In MACS, cells were revived in 0.1% phosphate-buffered saline (PBS; C0221A)-bovine serum albumin (BSA, ST2254) from Beyotime (Shanghai, China). They were then labeled with phycoerythrin (PE)-conjugated CD24 antibody (555428, BD-PharMingen, San Diego, CA, USA) and fluorescein isothiocyanate (FITC)-conjugated CD44 antibody (555478, BD-PharMingen, San Diego, CA, USA)-phosphate-buffered saline (PBS; C0221A, Beyotime, Shanghai, China). Employing the "DOUBLE POSITIVE SORT" program on the AutoMACS system (Miltenyi Biotech, Auburn, CA, USA), cell suspension was filtered and sorted. The positive and negative fractions for SP were evaluated and sorted with a FACSCalibur flow cytometer (Becton Dickenson, Mountain View, CA, USA).

2.3 RNA Extraction and Reverse Transcription Quantitative Polymerase Chain Reaction (RT-qPCR)

Following the directions of the maker, TRIzol reagent (R0016, Beyotime, Shanghai, China) was utilized to extract RNA. With a reverse transcription kit

(D7168S, Beyotime, Shanghai, China), 500 mg RNA was reversely transcribed into cDNA (10 µL). qPCR was conducted to quantitate lncRNAs MIR155HG and RelA on the Step One Plus Real-Time PCR System (Applied Biosystems, Foster City, CA, USA) using SYBR Premix Ex TaqTM II (Q331-02/03, Vazyme, Nanjing, China) in three independently repeated experiments. Expression analyses were achieved by $2^{-\Delta\Delta Ct}$ method. Sangon Biotech (Shanghai, China) created primers, with lncRNA MIR155HG forward the sequences below: (F), 5'-ACGGTTGTGCGAGCAGAGAATCTA-3' reverse (R), 5'-CTCATCTAAGCCTCACAACAACCT-RelA F, 5'-CTTCCTCAGCCATGGTACCTCT-3' 5'-CAAGTCTTCATCAGCATCAAACTG-3'; Glyceraldehyde 3-phosphate dehydrogenase (GAPDH) F, 5'-CCATGGGGAAGGTGAAGGTC-3' and R, 5'-AGTGATGGCATGGACTGTGG-3'.

2.4 Cell Transfection

MCF-7 and MDA-MB-231 stem cells were divided into the following groups: Blank, short hairpin RNA negative control (shNC), short hairpin RNA targeting MIR155HG (shMIR155HG), vector, RelA, shNC+vector, shMIR155HG+vector, shNC+RelA, and shMIR155HG+RelA. GenePharma (Shanghai, China) supplied shMIR155HG and shNC. The pcDNA3.1-RelA (RelA) and control empty vector plasmids (vector) were acquired from GeneChem (Shanghai, China). transfection with 1 µg shRNA or 2 µg plasmid was completed utilizing Lipofectamine 2000 (11668019, Invitrogen, Carlsbad, CA, USA) (48 h, 37 °C) for later trials. The sequences were as follows: shMIR155HG-1, 5'-GCAGATAACTTGTCTGCATTTCAAGAGAATGCAGA CAAGTTATCTGCTTTTTT-3'; shMIR155HG-2, GCATTCACATGGAACAAATTTCAAGAGAATTTGTT CCATGTGAATGCTTTTTT-3'; 5'-GCACCCAGTCCGCCCTGAGCAAATTCAAGAGATTT GCTCAGGGCGGACTGGGTGCTTTTT-3'.

2.5 Colony Formation Assay

Equal densities of cells were planted onto 60 mm cell culture dishes, and cultured for 4–10 h (37 °C) to promote adhesion. Following that, cells received X-ray radiation (0, 2, 4, and 6 Gy) utilizing an RS2000 X-ray biological research irradiator (Rad Source Technologies, Suwanee, GA, USA) [21]. To facilitate colony development, cell incubation was conducted for 10–14 days. The colonies underwent fixation (methanol, 322415, Sigma-Aldrich, St. Louis, MO, USA) and staining (0.1% crystal violet; C0121, Beyotime, Shanghai, China). At least fifty cells in a colony were counted. Surviving fraction = the number of colonies/(cells inoculated × plating efficiency).

2.6 Western Blot Analysis

Using lysis buffer (KGC4901; Keygene, Jiangsu, China), total protein from the cells was determined via BCA



protein assay kit (P0010; Beyotime, Shanghai, China). For sodium dodecyl sulfate polyacrylamide gel electropheresis (SDS-PAGE, KGC4901; Keygene, Jiangsu, China), 40 μg of protein per lane was loaded and separated on 10% gels, followed by being transferred onto polyvinylidene fluoride (PVDF) membranes (KGC4806; Keygene, Jiangsu, China). Membranes experienced 1-h blockage at room temperature (RT) using 5% non-fat milk in Tris-Buffered Saline with Tween-20 (TBST, ST825; Beyotime, Shanghai, China), and cultivation with primary antibodies (4 °C, overnight) obtainable from Abcam (Cambridge, UK) except RelA (65 kDa; 1:1000, AM06378SU-N, Origene, Rockville, MD, USA), incorporating β -catenin (85 kDa; 1:400, ab224803), Nanog (37 kDa; 1:1000, ab109250), SRY-Box transcription factor 2 (SOX2, 35 kDa; 1:1000, ab92494), phosphorylated histone variant H2A.X (γ H2A-X, 15 kDa; 1:5000, ab81299), BCL2-Associated X Protein (Bax, 21 kDa; 1:1000, ab32503), B-cell lymphoma-2 (Bcl-2, 26 kDa; 1:2000, ab182858), Cleaved Caspase 3 (17 kDa; 1:500, ab32042), Caspase 3 (35 kDa; 1:5000, ab32351), and GAPDH (36 kDa; 1:1000, ab8245). Next, membranes were incubated (1 h, RT) with horseradish peroxidase (HRP)-conjugated secondary antibodies (Abcam, Cambridge, UK), Goat Anti-Mouse Immunoglobulin G (IgG, ab205719; 1:2000)/Goat Anti-Rabbit IgG (ab6721; 1:2000). Using gel imaging equipment (Chemi Doc MP, Bio-Rad, Hercules, CA, USA), protein bands were observed through the Pierce ECL Plus Western Blotting Substrate (KGC4902; Keygene, Jiangsu, China). With GAPDH as the loading control and ImageJ 5.2.1 software (NIH, Bethesda, MD, USA), protein production was measured and normalized.

2.7 Immunofluorescence Assay

Cells were seeded at equal densities onto glass slides and incubated (37 °C, 4-10 h) to allow for attachment. After that, cells underwent exposure to 2 Gy X-rays for 24 h. Immunofluorescence staining was carried out employing a DNA damage detection kit (7H2A-X Immunofluorescence Assay) (C2036S; Beyotime, Shanghai, China) in compliance with the guidelines. Simply put, PBSwashed cells were fixed with fixative (15 min; C2036S-1, Beyotime, Shanghai, China), blocked with blocking solution (20 min; C2036S-3, Beyotime, Shanghai, China), and incubated with γ H2A-X antibody (1:250; C2036S-4, Beyotime, Shanghai, China) (4 °C, overnight), and rabbit Cy3 secondary antibody (1:500; C2036S-5, Beyotime, Shanghai, China) (RT, 1 h). After washing, cell nucleus was stained with 4,6-diamino-2-phenyl indole (DAPI) (5 min, RT; C2036S-6, Beyotime, Shanghai, China), and images were obtained employing FluoViewTM FV1000 confocal laser scanning microscope (200×, Olympus, Tokyo, Japan).

2.8 Sphere Formation Assay

With the goal to create spheres, single-cell suspensions (30,000 cells/well) were cultivated in serum-free Minimum Essential Medium (MEM, 11058021) with 20 ng/mL bFGF, 20 ng/mL EGF, and B27 (all from Thermo Fisher Scientific, Waltham, MA, USA) in 100 mm ultra-low attachment plates (4615, Corning Inc., Corning, NY, USA). The development of spheres was captured by an inverted microscope (200×, Olympus, Tokyo, Japan).

2.9 Cell Apoptosis and Cell Cycle Analysis

Following 24-h exposure to 2 Gy X-rays, cells experienced color development by Annexin V-FITC and PI (FITC Annexin V Apoptosis Detection Kit, C1062S, Beyotime, Shanghai, China), followed by cell cycle analysis exploiting TaliTM Cell Cycle Kit (A10798, Thermo Fisher Scientific, Waltham, MA, USA). Measurements of apoptosis and cell cycle were completed utilizing a flow cytometer, follows by result evaluation with CellQuest software (version 5.1, BD Biosciences, San Jose, CA, USA).

2.10 Prediction of Transcription Factor-Binding Motifs and Dual-Luciferase Reporter Assay

Transcription factor-binding motifs were predicted using the JASPAR database (https://jaspar.elixir.no/). MIR155HG-wild type (WT) and mutant (MUT) sequences (wild and mutated sequences of the binding site between MIR155HG and RELA) were cloned into a luciferase reporter vector (16147, Promega, Madison, WI, USA). With Lipofectamine 2000, MIR155HG-WT or MIR155HG-MUT and RELA were co-transfected into MDA-MB-231 and MCF-7 stem cells. Overnight cell lysis was followed by luciferase activity assessment employing a luminometer (Bio-Rad, Hercules, CA, USA) and a Dual-Luciferase Reporter Assay Kit (E1910, Promega, Madison, WI, USA).

2.11 Chromatin Immunoprecipitation (ChIP)

ChIP Assay Kit (17-295, Millipore, Temecula, CA, USA) was purchased in advance. Briefly, cells were lysed on ice for 10 min. To extract 200–1000 bp DNA fragments from cell lysates, cells underwent seven times of 5-second pulses on ice with a Sonicator 3000 (Misonix, Farmingdale, NY, USA). An agarose bead mixture, ChIP buffer, and a protease inhibitor cocktail were used to pre-clear cell lysates for 1 h on ice. The lysates were treated (12 h, 4 °C) with either normal rabbit IgG (2729, 1:50) or RelA antibody (8242, 1:100) from Cell Signaling Technology (Danvers, MA, USA). The supernatant containing 60 μL Protein A Agarose/Salmon Sperm DNA was added and spun (1 h, 4 °C). Wash buffers containing low salt (150 mM), high salt (500 mM), LiCl, and TE buffer were applied to wash the beads. After elution of the complexes using elution buffer, 5 M NaCl was used to reverse the cross-links, and the mixture experienced 4-h incubation (65 °C). Following RNase A treatment, samples were collected for qPCR to gauge the



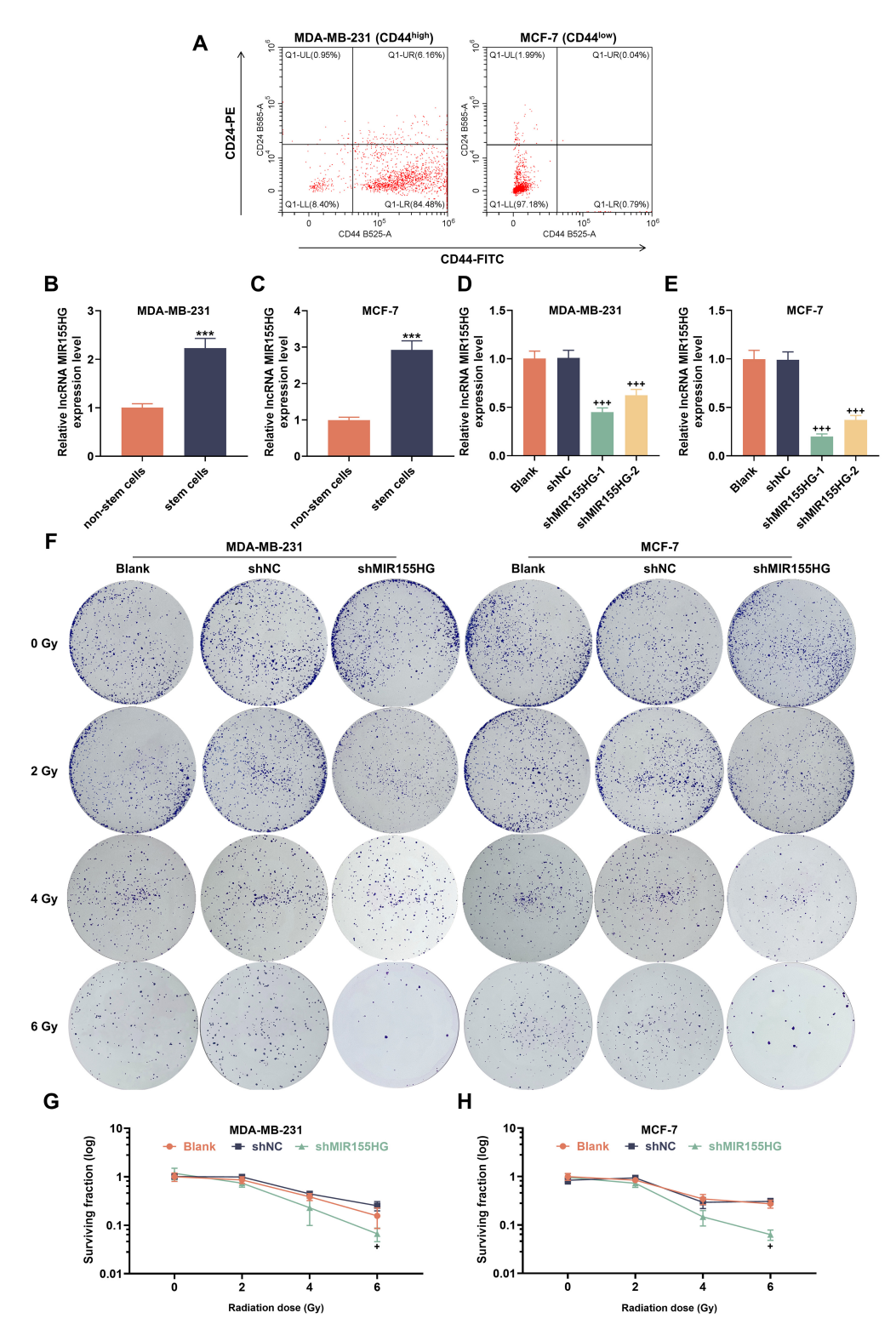


Fig. 1. Long non-coding RNA MIR155HG is highly expressed in Breast cancer stem cells (BCSCs), and knockdown of MIR155HG reduces cellular radioresistance. (A) FITC-CD44- and PE-CD24-stained MDA-MB-231 and MCF-7 cells (flow cytometry). (B,C) MIR155HG messenger RNA (mRNA) levels in MDA-MB-231 and MCF-7 stem and non-stem cells (reverse transcription quantitative polymerase chain reaction (RT-qPCR)). (D,E) MIR155HG mRNA levels in short hairpin RNA targeting MIR155HG (sh-MIR155HG)-transfected MCF-7 and MDA-MB-231 stem cells (RT-qPCR). (F) Representative images of MIR155HG-silencing MDA-MB-231 and MCF-7 stem cells under radiation (colony formation assays). (G,H) Survival curves of MIR155HG-silencing MDA-MB-231 and MCF-7 stem cells under radiation. n = 3. ***p < 0.001 compared to non-stem cells. p < 0.05, p < 0.001 compared to short hairpin RNA negative control (shNC).

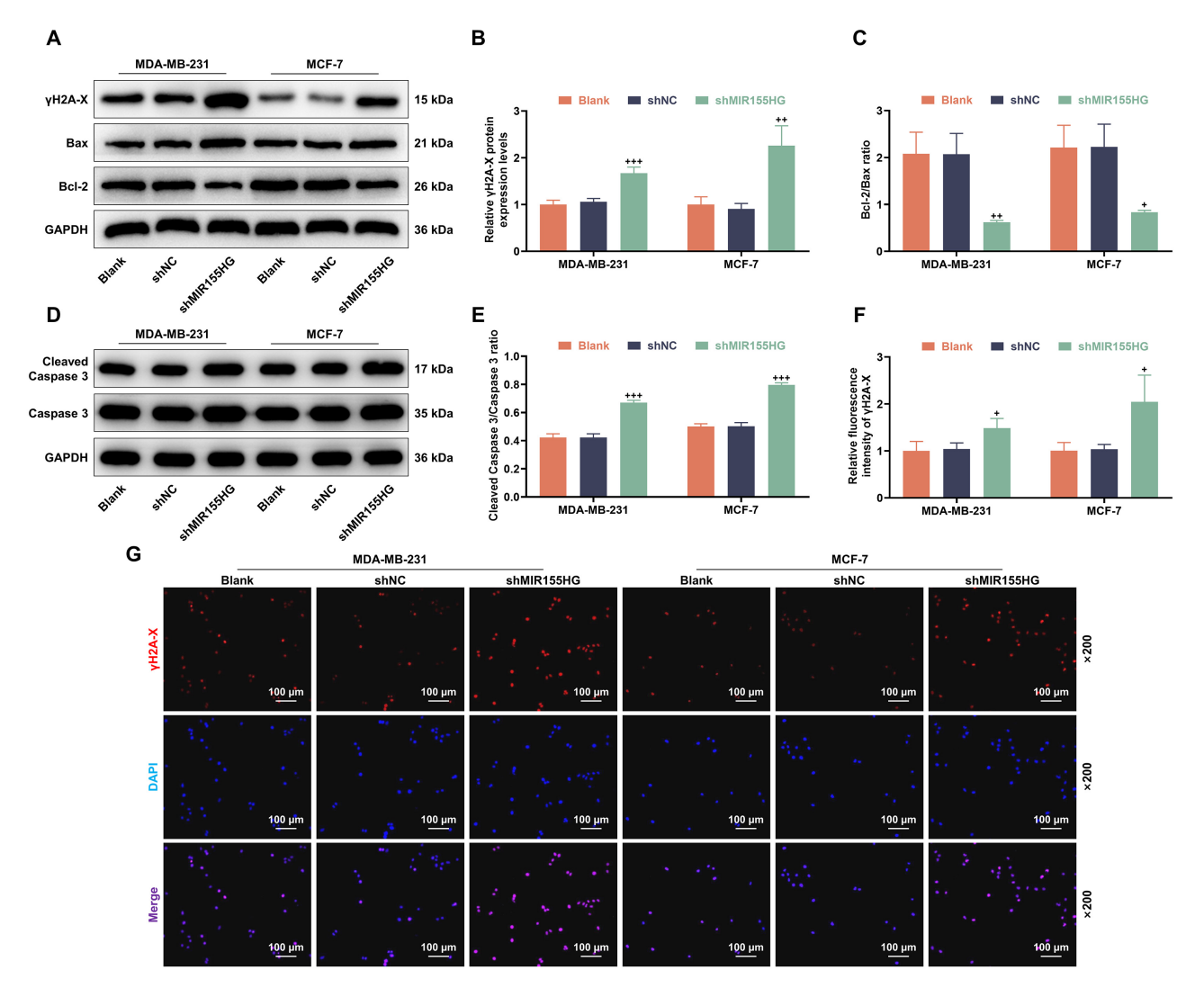


Fig. 2. Knockdown of *MIR155HG* reduces DNA damage repair and promotes apoptosis protein expression in BCSCs. (A–E) Phosphorylated histone variant H2A.X (γ H2A-X), BCL2-Associated X Protein (Bax), B-cell lymphoma-2 (Bcl-2), Caspase 3 and Cleaved Caspase 3 protein levels in sh-MIR155HG-transfected MCF-7 and MDA-MB-231 stem cells after 2 Gy X-ray irradiation for 24 h (Western blot, Glyceraldehyde 3-phosphate dehydrogenase (GAPDH) as an internal control). (F,G) γ H2A-X levels in sh-MIR155HG-transfected MCF-7 and MDA-MB-231 stem cells after 2 Gy X-ray irradiation for 24 h (Immunofluorescence). Red fluorescence represents γ H2A-X and blue fluorescence indicates DAPI cell nuclear staining. Magnification 200×, scale bar 100 μ m. n = 3. ^+p < 0.05, ^{++}p < 0.01, ^{+++}p < 0.001 compared to shNC.

levels of the *MIR155HG* promoter. The primer sequences used were F 5'-GGTCTCCAGCTGATTCGGTC-3' and R 5'-CCAGGAGCGTCTCCTTGGTT-3'.

2.12 Statistical Analysis

Each experiment was independently repeated three times. Statistical studies were carried out with the aid of GraphPad Prism 8.0 (GraphPad Software, Boston, MA, USA). Data were displayed as mean \pm standard deviation (SD). Two-group and multi-group comparisons were accomplished utilizing an independent sample t-test, and oneway or two-way ANOVA followed by Tukey's post-hoc test, respectively. p < 0.05 reflected statistically significant differences.

3. Results

3.1 MIR155HG Level is Raised in BCSCs and MIR155HG Knockdown Enhances Cellular Radiosensitivity

Through flow cytometry, we first separated stem cells from breast cancer cell lines, and detected CD44 $^+$ /CD24 $^-$ cells >80% in MDA-MB-231 cells and <10% in MCF-7 cells (Fig. 1A). Next, we performed RT-qPCR to ascertain *MIR155HG* expression level in stem and non-stem cells. *MIR155HG* mRNA expression was greater in BCSCs than non-stem cells, according to RT-qPCR data (p < 0.001, Fig. 1B,C). Next, MDA-MB-231 and MCF-7 stem cells were transfected with shMIR155HG-1 and shMIR155HG-2 to knock down *MIR155HG*, where *MIR155HG* expression was confirmed to be decreased (p < 0.001, Fig. 1D,E).



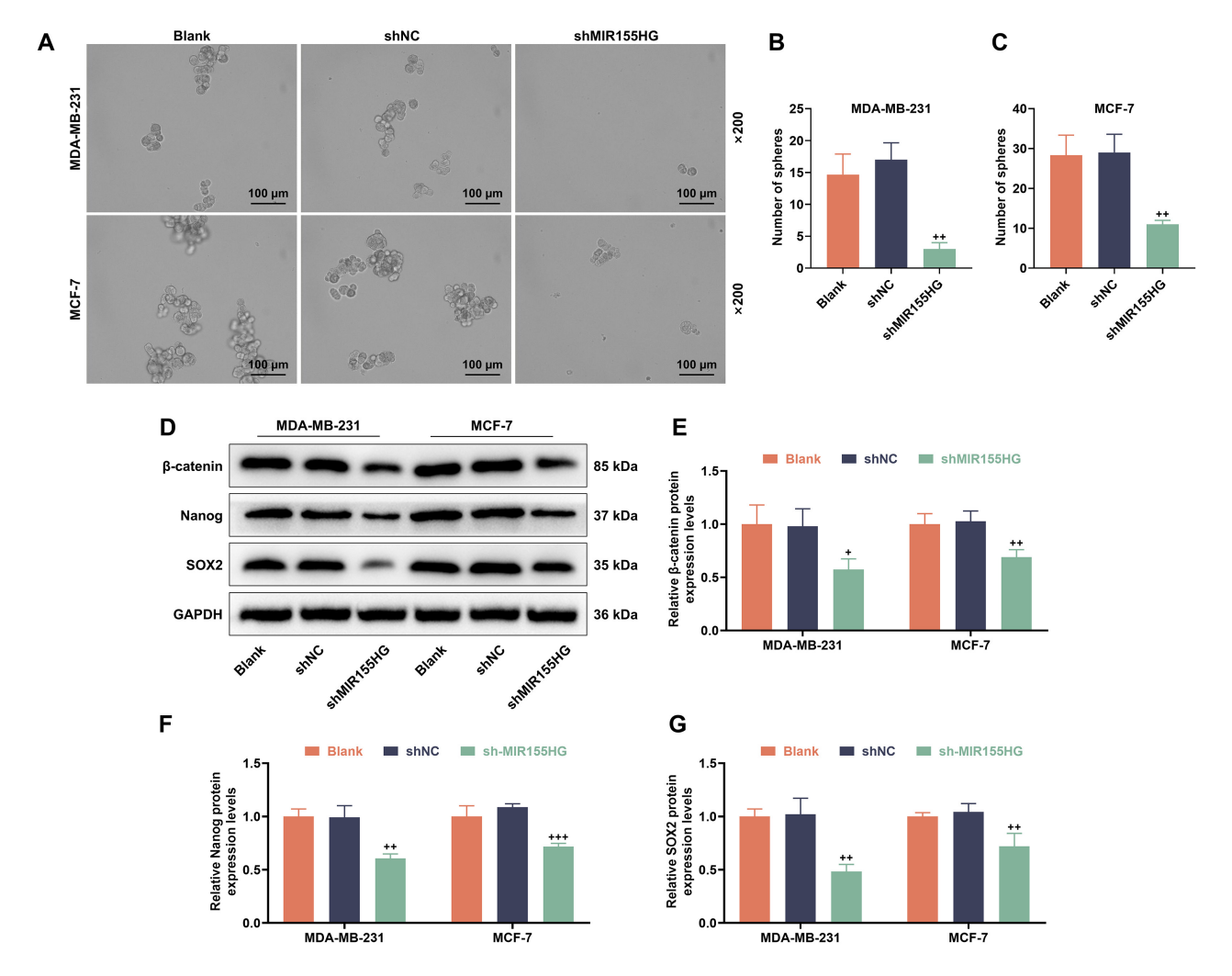


Fig. 3. Knockdown of *MIR155HG* reduces stemness and inhibits Wnt-related protein expression in BCSCs. (A–C) Stemness in sh-MIR155HG-transfected MCF-7 and MDA-MB-231 stem cells after 2 Gy X-ray irradiation for 24 h (Sphere formation assay). Magnification $200\times$, scale bar $100~\mu m$. (D–G) β -catenin, Nanog, and SRY-Box transcription factor 2 (SOX2) protein levels in sh-MIR155HG-transfected MCF-7 and MDA-MB-231 stem cells after 2 Gy X-ray irradiation for 24 h (western blot, GAPDH as an internal control). n = 3. p < 0.05, p < 0.05, p < 0.01, p

The shMIR155HG-1, which exhibited the most evident knockdown efficacy, was selected for further experiments. Different radiation dosages were applied to these cell lines, colony formation assay confirmed knockdown of *MIR155HG* conferred greater sensitivity to X-rays irradiation treatment in the *MIR155HG*-knockout MDA-MB-231 and MCF-7 stem cells compared to their parental cells (Fig. 1F–H). Combined with reference to a previous study [21], 2 Gy X-rays was selected for the following experiment.

3.2 Knockdown of MIR155HG Reduces DNA Damage Repair and Promotes Apoptotic Protein Expression in BCSCs

One day after 2 Gy X-ray irradiation, we detected the expression of γ H2A-X, a significant effector of DNA damage, in MDA-MB-231 and MCF-7 stem cells to clarify how *MIR155HG* increases radioresistance in stem cells. Based

on Western blot data, MIR155HG knockdown resulted in higher γ H2A-X protein levels (p < 0.01, Fig. 2A,B), as well as lower levels of Bcl-2/Bax (p < 0.05, Fig. 2C) and higher levels of Cleaved Caspase 3/Caspase 3 proteins (p < 0.001, Fig. 2D,E). Immunofluorescence staining results suggested that MIR155HG knockdown was associated with higher amounts of γ H2A-X (red) (p < 0.05, Fig. 2F,G).

3.3 Knockdown of MIR155HG Reduces Stemness and Suppresses Wnt-Related Protein Expression in BCSCs

Next, following 2 Gy X-ray irradiation, we assessed the development of tumor spheres in MDA-MB-231 and MCF-7 stem cells. The tumor sphere-forming ability was weaker in sh-MIR155HG group than shNC group (p < 0.01, Fig. 3A–C). Additionally, β -catenin, Nanog, and SOX2 protein levels were lower in sh-MIR155HG group versus shNC group (p < 0.05, Fig. 3D–G).



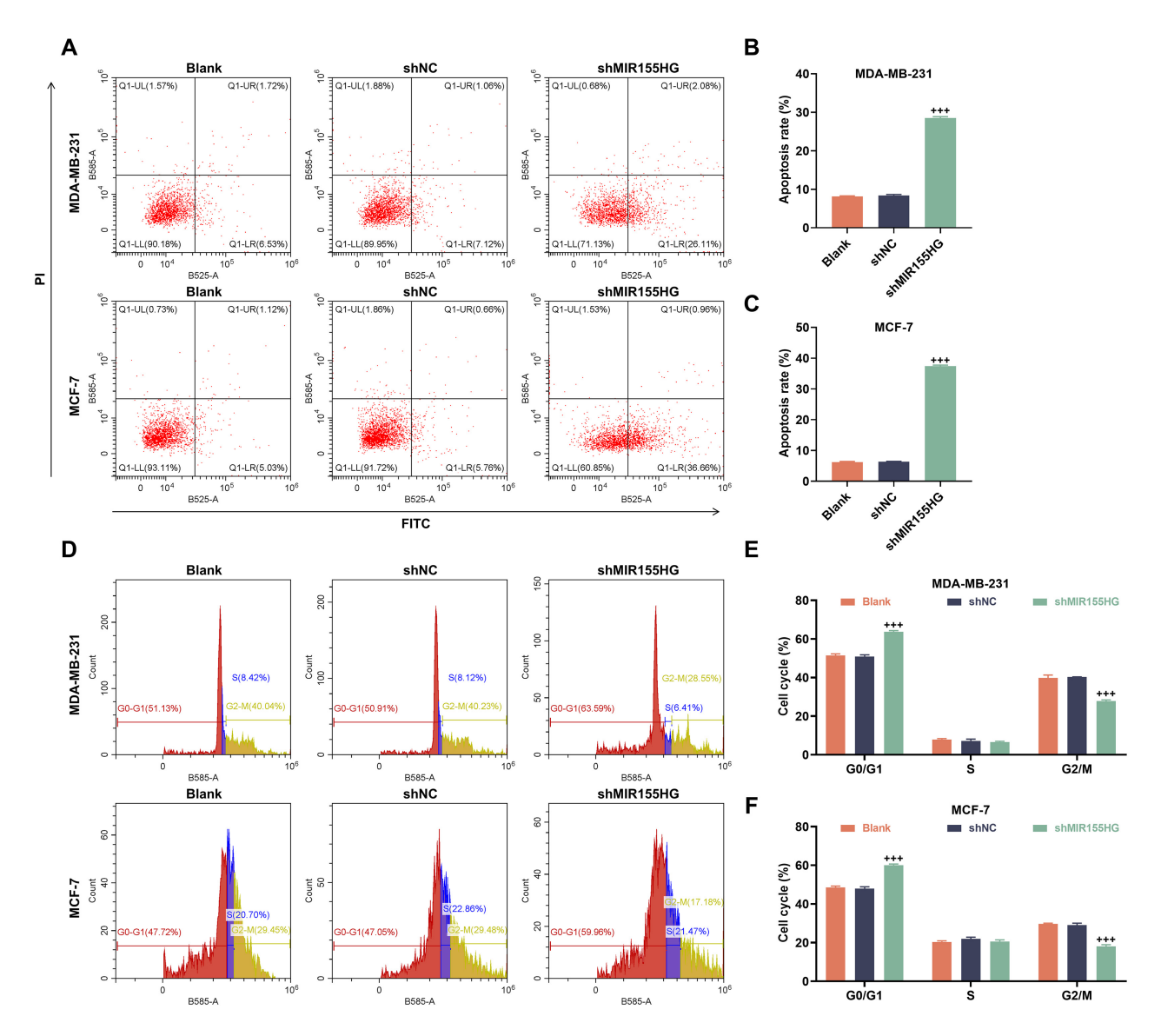


Fig. 4. Knockdown of *MIR155HG* promotes apoptosis and induces G1 phase arrest in BCSCs. (A–C) Apoptosis in sh-MIR155HG-transfected MCF-7 and MDA-MB-231 stem cells after 2 Gy X-ray irradiation for 24 h (flow cytometry). (D–F) Cell cycle in sh-MIR155HG-transfected MCF-7 and MDA-MB-231 stem cells after 2 Gy X-ray irradiation for 24 h (flow cytometry). n = 3. ^{+++}p < 0.001 compared to shNC.

3.4 Knockdown of MIR155HG Promotes Apoptosis and Induces G1 Phase Arrest in BCSCs

To further assess whether *MIR155HG* regulates cellular apoptosis and cycle induction in response to radiation, we examined apoptosis and cell cycle profiles in MDA-MB-231 and MCF-7 stem cells after X-ray irradiation (2 Gy). Sh-MIR155HG group exhibited increased apoptosis (p < 0.001, Fig. 4A–C), as well as a decrement in G2 phase cells and increment in G0/G1 phase cells (p < 0.001, Fig. 4D–F).

3.5 NF-&B Subunit RelA Binds to the MIR155HG Promoter Region and Promotes its Transcriptional Function

By means of JASPAR analysis, we identified four potential binding sites for the NF- κ B subunit *RelA* within the

MIR155HG promoter region. Among them, the site located at -1828/-1837 showed higher score in JASPAR analysis and was used for subsequent analysis (Fig. 5A,B). Furthermore, *RelA* significantly enhanced luciferase activity in *MIR155HG*-WT cells (p < 0.001, Fig. 5C,D). ChIP analysis confirmed the binding of *RelA* to *MIR155HG* promoter (p < 0.001, Fig. 5E). Overexpression of *RelA* markedly upregulated *RelA* levels in stem cells (p < 0.001, Fig. 5F–I).

3.6 NF-κB Subunit RelA Enhances DNA Damage Repair and Suppresses Apoptotic Protein Expression via Upregulating MIR155HG in BCSCs

Following 2 Gy X-ray treatment for 24 h, colony survival rates were reduced in the shMIR155HG+vector group, but were elevated in the shNC+RelA group (p < 0.05, Fig. 6A–C). In the shMIR155HG+RelA group,



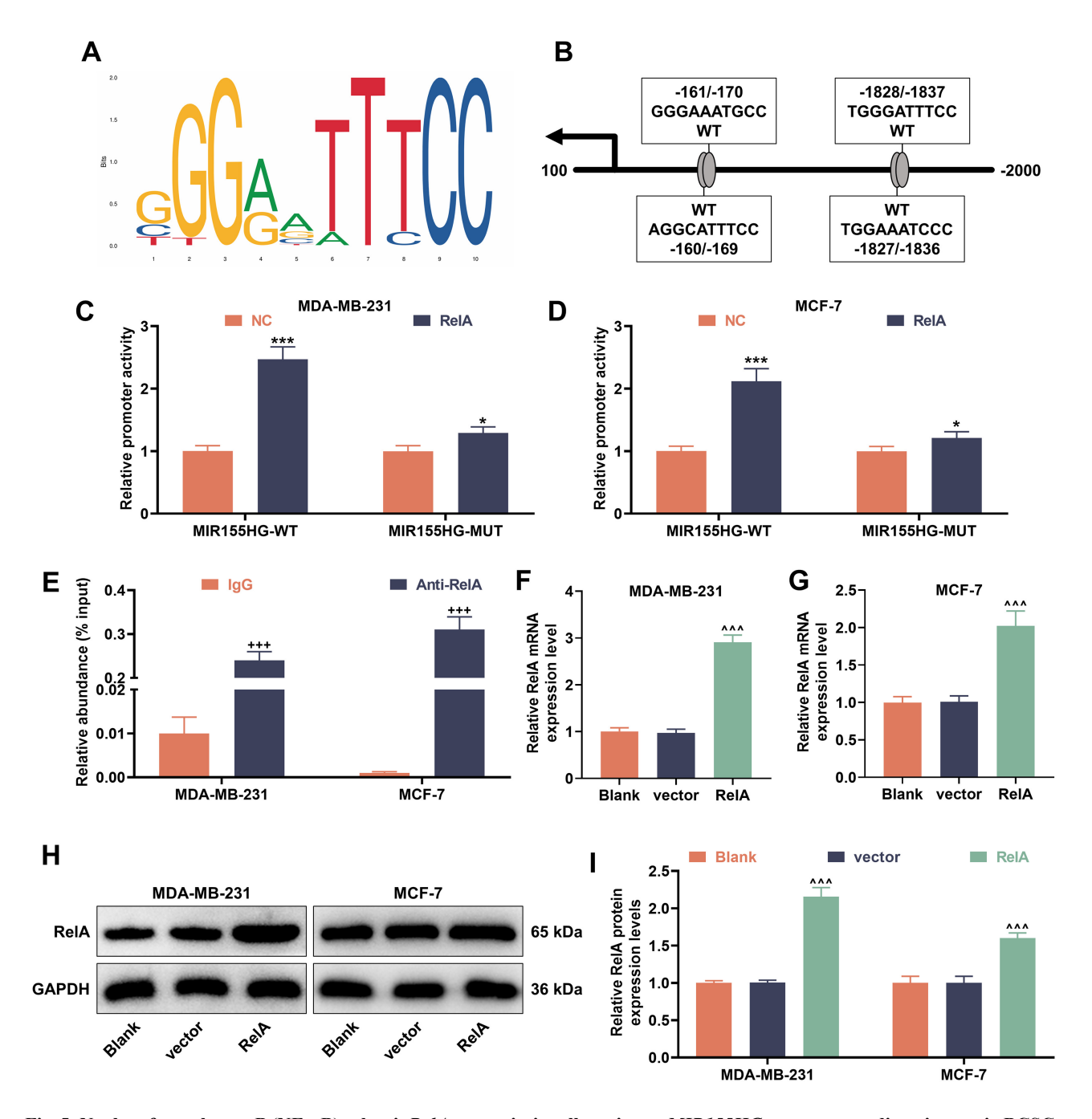


Fig. 5. Nuclear factor kappa B (NF- κ B) subunit *RelA* transcriptionally activates *MIR155HG* to promote radioresistance in BCSCs. (A) *RelA* binding motifs (JASPAR analysis). (B) Potential binding sequences between *RelA* and the *MIR155HG* promoter (JASPAR prediction). (C,D) Luciferase activity in MCF-7 and MDA-MB-231 stem cells with *RelA* overexpression at the *MIR155HG* promoter (Dual-luciferase reporter gene assay). (E) Interaction between *RelA* and *MIR155HG* promoter (Chromatin immunoprecipitation (ChIP) assay). (F–I) *RelA* expression in MCF-7 and MDA-MB-231 stem cells overexpressing *RelA* (RT-qPCR and western blot). n = 3. *p < 0.05, ***p < 0.001 compared to NC. ++++p < 0.001 compared to immunoglobulin G (IgG). ^^^p < 0.001 compared to vector.

colony survival rates were greater than those in the shMIR155HG+vector group but lower than those in the shNC+RelA group (p < 0.05, Fig. 6A–C). Following 2 Gy X-ray treatment for 24 h, compared to the shNC+vector group, MDA-MB-231 and MCF-7 stem cells in the shMIR155HG+vector group had upregulated γ H2A-X and Cleaved Caspase 3/Caspase 3 protein, and downregulated

Bcl-2/Bax (p < 0.05, Fig. 6D–H). Conversely, in the shNC+RelA group, protein levels of γ H2A-X and Cleaved Caspase 3/Caspase 3 declined, while Bcl-2/Bax levels rose (p < 0.05, Fig. 6D–H). In the shMIR155HG+RelA group, γ H2A-X and Cleaved Caspase 3/Caspase 3 proteins levels were lower than those in the shMIR155HG+vector group but greater than those in the shNC+RelA group,



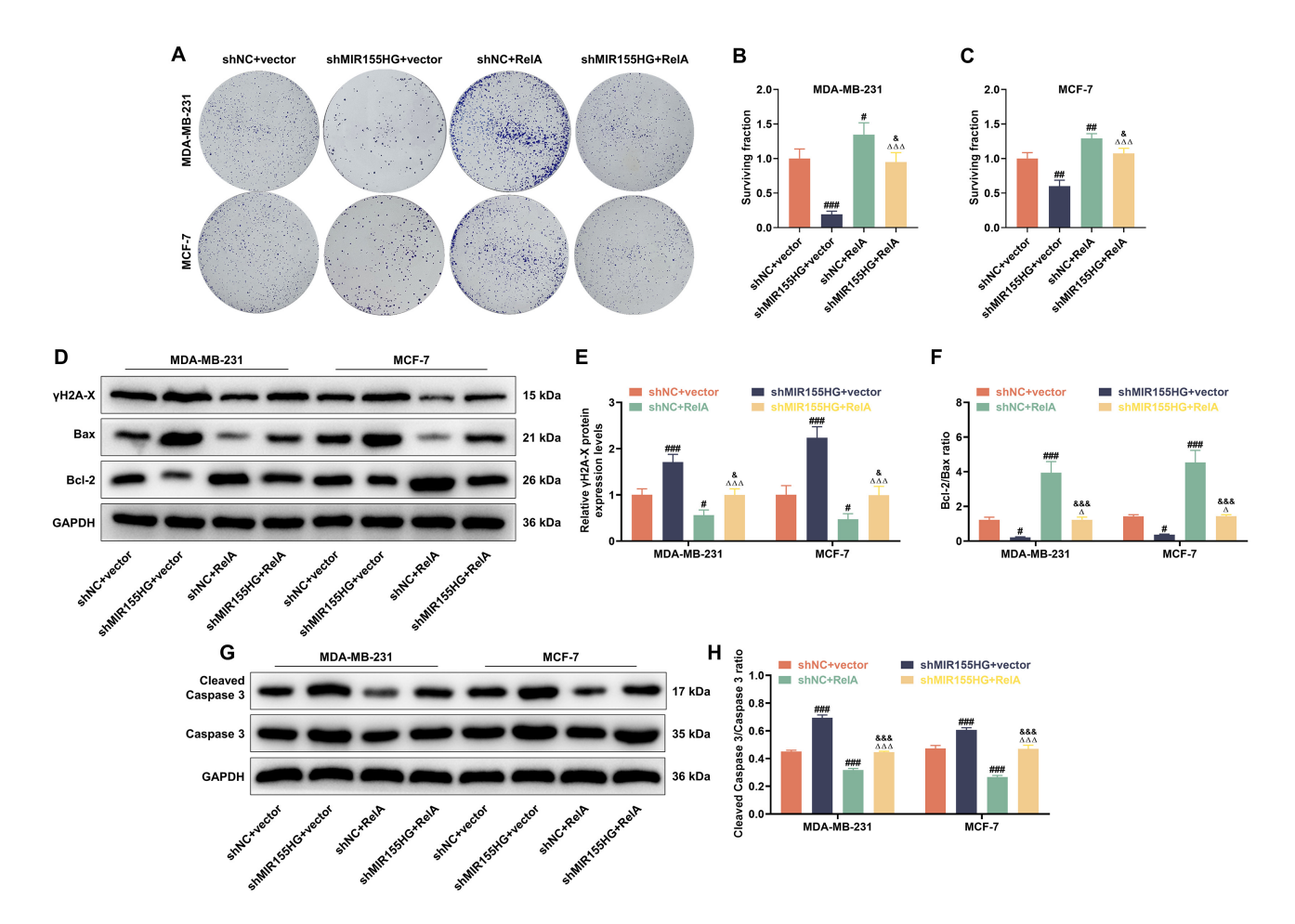


Fig. 6. NF- κ B subunit *RelA* upregulates *MIR155HG* to inhibit γ H2A-X and apoptosis-related protein expression in BCSCs. (A–C) Representative images of survival rates of MDA-MB-231 and MCF-7 stem cells in shNC+vector, shMIR155HG+vector, shNC+RelA, and shMIR155HG+RelA groups after 2 Gy X-ray treatment for 24 h (colony formation assay). (D–H) γ H2A-X, Bax, Bcl-2, Caspase 3, and Cleaved Caspase 3 protein expressions in MDA-MB-231 and MCF-7 stem cells in shNC+vector, shMIR155HG+vector, shNC+RelA, and shMIR155HG+RelA groups after 2 Gy X-ray treatment for 24 h (western blot). n = 3. $^{\#}p < 0.05$, $^{\#\#}p < 0.01$, $^{\#\#}p < 0.001$ compared to shNC+vector. $^{\Delta}p < 0.05$, $^{\Delta\Delta\Delta}p < 0.001$ compared to shMIR155HG+vector. $^{\&}p < 0.05$, $^{\&\&\&}p < 0.001$ compared to shNC+RelA.

while the opposite trends were detected in the levels of Bcl-2/Bax (p < 0.05, Fig. 6D–H). Immunofluorescence staining results confirmed γ H2A-X (red) in stem cells was increased in the shMIR155HG+vector group (p < 0.001, Fig. 7A–C), yet decreased in the shNC+RelA group (Fig. 7A–C), compared to the shNC+vector group. In the shMIR155HG+RelA group, γ H2A-X levels were higher than those in the shNC+RelA group (p < 0.05), but lower than those in the shMIR155HG+vector group (p < 0.001, Fig. 7A–C).

3.7 NF-kB Subunit RelA Enhances Stemness and Promotes Wnt-Related Protein Expression via Upregulating MIR155HG in BCSCs

Sphere formation assays revealed that following 2 Gy X-ray treatment for 24 h, tumor sphere was reduced in shMIR155HG+vector group yet increased in shNC+RelA group (p < 0.05, Fig. 8A–C). Tumor sphere formation ability was potentiated in shNC+RelA group relative to

shNC+vector group, but weakened in shMIR155HG+RelA group compared to shNC+RelA group (p < 0.05, Fig. 8A–C). Western blot data revealed in contrast to shNC+vector group, the expressions of β -catenin, Nanog, and SOX2 were decreased in shMIR155HG+vector group yet increased in shNC+RelA group (p < 0.05, Fig. 8D–G). These protein levels in shMIR155HG+RelA group were higher than those in shMIR155HG+vector group, but lower than those in shNC+RelA group (p < 0.05, Fig. 8D–G).

3.8 Silencing of LncRNA MIR155HG Reverses NF- κ B Subunit RelA-induces Inhibition of Apoptosis and G1 Phase Arrest

Flow cytometry analysis showed that following 2 Gy X-ray treatment for 24 h, apoptosis was facilitated in stem cells in shMIR155HG+vector group, but dampened in shNC+RelA group (p < 0.01, Fig. 9A–C). Relative to shMIR155HG+RelA group, shNC+RelA group had weaker while shMIR155HG+vector group had stronger apopto-



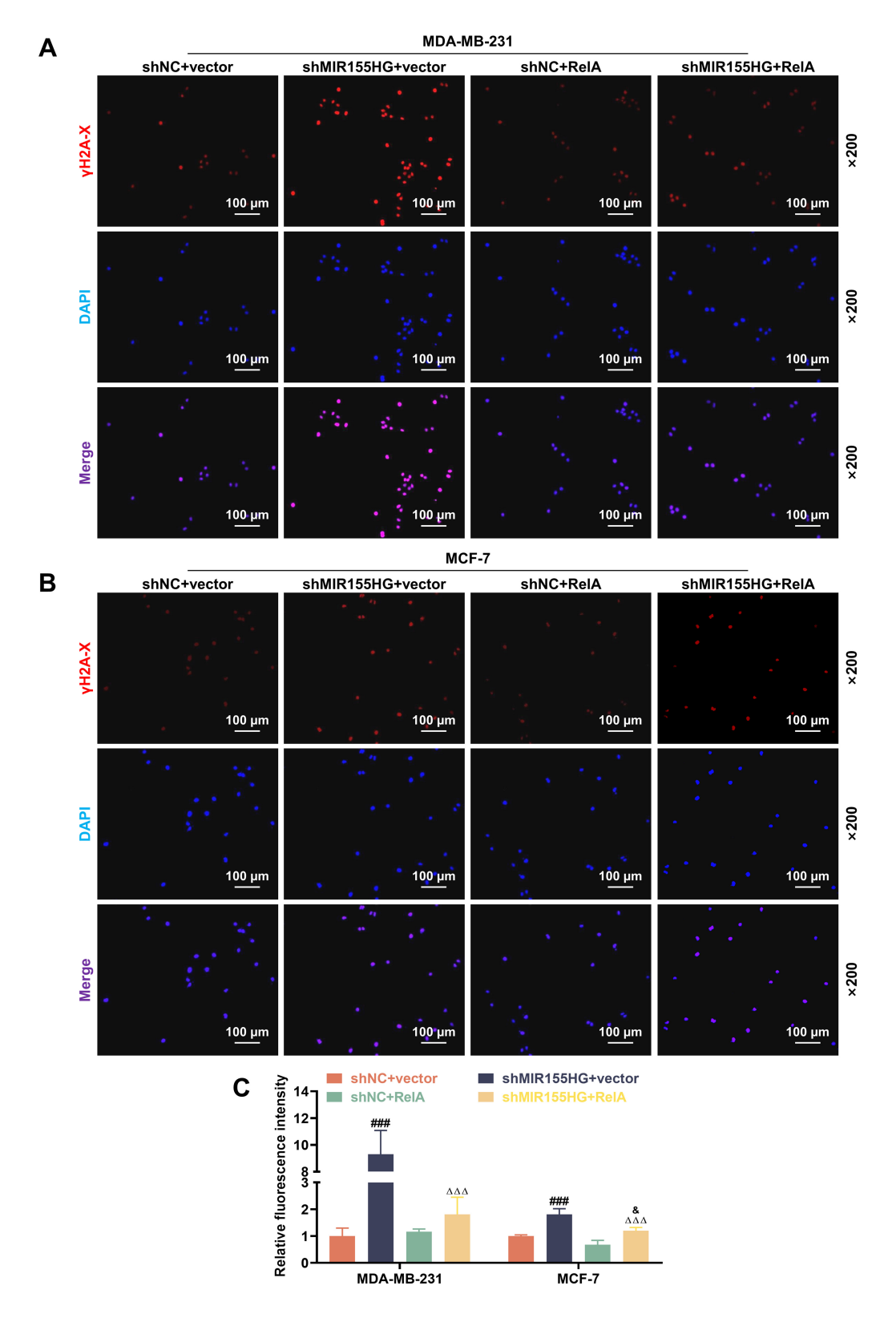


Fig. 7. NF- κ B subunit *RelA* upregulates *MIR155HG* to promote DNA damage repair in BCSCs. (A–C) γ H2A-X levels in MDA-MB-231 and MCF-7 cells in shNC+vector, shMIR155HG+vector, shNC+RelA, and shMIR155HG+RelA groups after 2 Gy X-ray treatment for 24 h (Immunofluorescence). Red fluorescence represents γ H2A-X and blue fluorescence indicates DAPI cell nuclear staining. Magnification 200×, scale bar 100 μ m. n = 3. **##p < 0.001 compared to shNC+vector. *\(^{\Delta\Delta}p < 0.001 compared to shMIR155HG+vector. *\(^{\Delta}p < 0.05 compared to shNC+RelA.

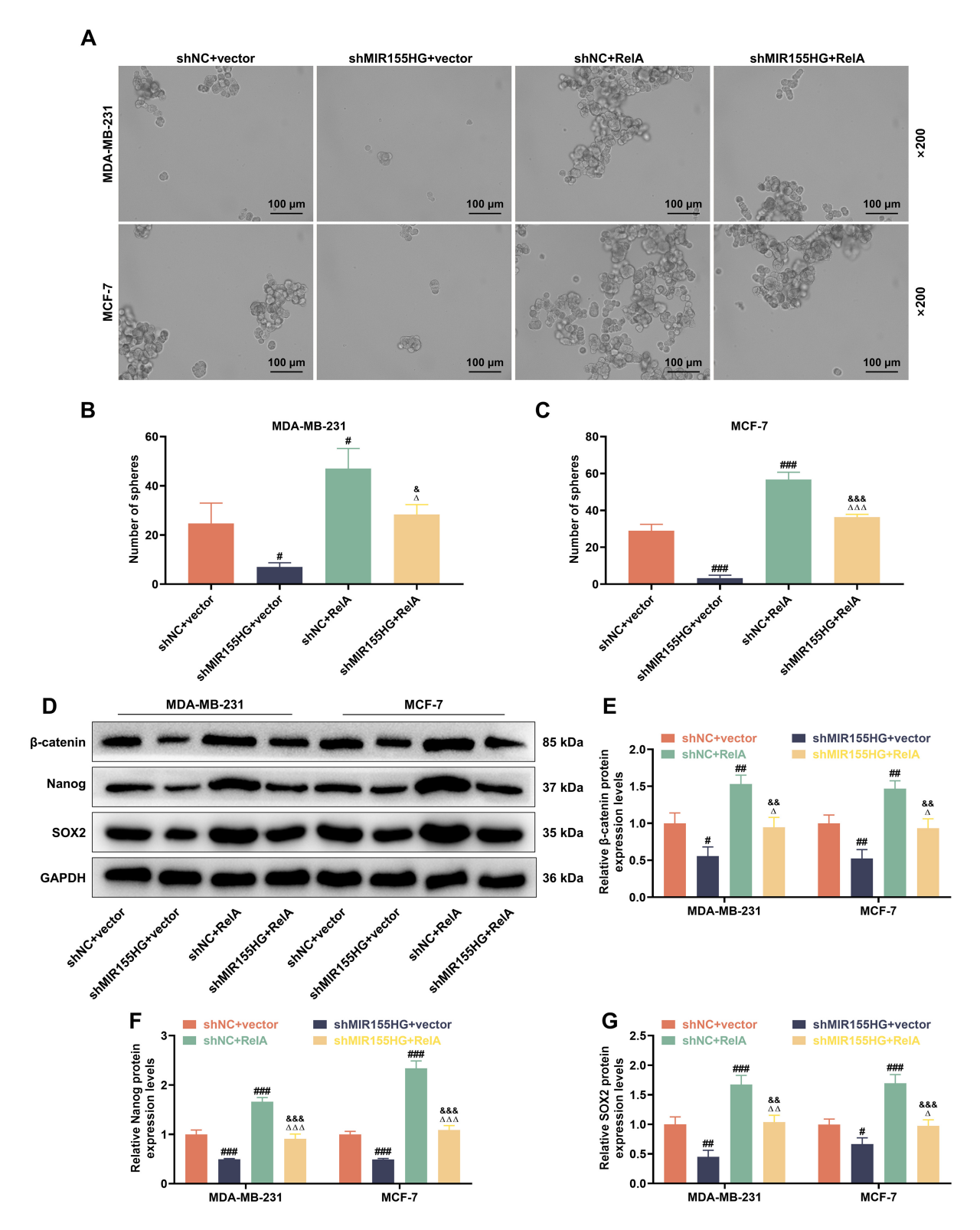


Fig. 8. MIR155HG Knockdown reverses NF- κ B subunit RelA-induced stemness and regulates Wnt-related protein expression in BCSCs. (A–C) Stemness in MDA-MB-231 and MCF-7 cells in shNC+vector, shMIR155HG+vector, shNC+RelA, and shMIR155HG+RelA groups after 2 Gy X-ray treatment for 24 h (sphere formation assay). Magnification 200×, scale bar 100 μm. (D–G) β -catenin (E), Nanog (F), and SOX2 (G) protein expressions in MDA-MB-231 and MCF-7 stem cells in shNC+vector, shMIR155HG+vector, shNC+RelA, and shMIR155HG+RelA groups after 2 Gy X-ray treatment for 24 h (western blot, GAPDH as an internal control). n = 3. $^{\#}p < 0.05$, $^{\#}p < 0.01$, $^{\#}p < 0.001$ compared to shNC+vector. $^{\Delta}p < 0.05$, $^{\Delta\Delta}p < 0.01$, $^{\Delta\Delta\Delta}p < 0.001$ compared to shNIR155HG+vector. $^{\Phi}p < 0.05$, $^{\&\Phi}p < 0.01$, $^{\&\&\Phi}p < 0.001$ compared to shNC+RelA.

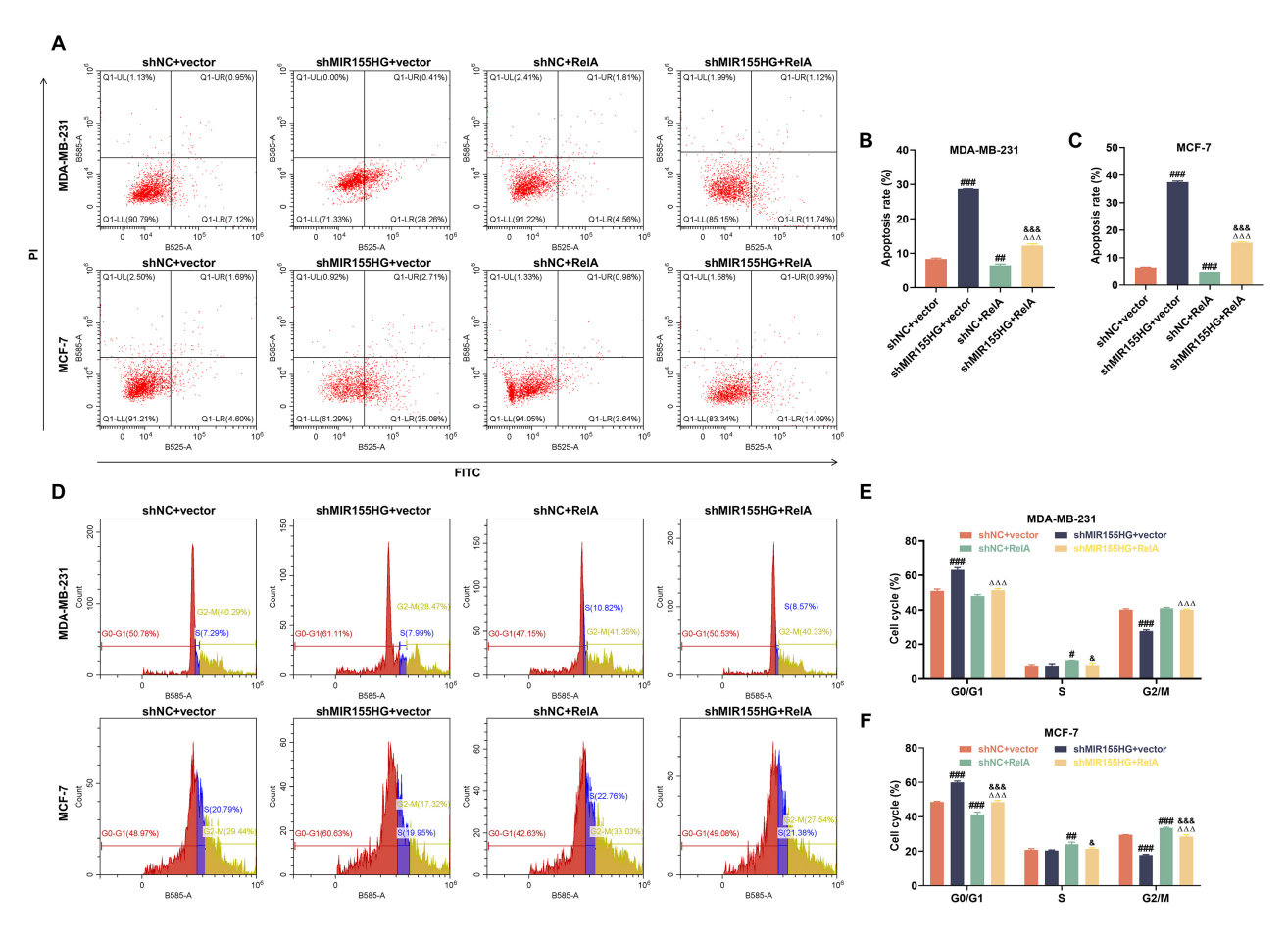


Fig. 9. MIR155HG knockdown reverses NF- κ B subunit RelA-suppressed apoptosis and G1 phase arrest in BCSCs. (A–C) Apoptosis in MDA-MB-231 and MCF-7 cells in shNC+vector, shMIR155HG+vector, shNC+RelA, and shMIR155HG+RelA groups after 2 Gy X-ray treatment for 24 h (flow cytometry). (D–F) Cell cycle in MDA-MB-231 and MCF-7 stem cells in shNC+vector, shMIR155HG+vector, shNC+RelA, and shMIR155HG+RelA groups after 2 Gy X-ray treatment for 24 h (Flow cytometry). Each experiment was independently repeated three times. $^{\#}p < 0.05$, $^{\#\#}p < 0.01$, $^{\#\#}p < 0.001$ compared to shNC+vector. $^{\Delta\Delta\Delta}p < 0.001$ compared to shMIR155HG+vector. $^{\&}p < 0.05$, $^{\&\&\&}p < 0.001$ compared to shNC+RelA.

sis ability (p < 0.001, Fig. 9A–C). MDA-MB-231 stem cells in the shMIR155HG+vector group had more G0/G1 phase cells and less G2/M phase cells in comparison to the shNC+vector group; in contrast, the shNC+RelA group displayed more S phase cells (p < 0.05, Fig. 9D,E). Compared to shMIR155HG+RelA group, shMIR155HG+vector group had more cells in the G0/G1 phase and less cells in the G2/M phase (p < 0.001, Fig. 9D,E); similarly, cells in the S phase were more in shNC+RelA group (p < 0.05, Fig. 9D,E). In the shMIR155HG+vector group, MCF-7 stem cells displayed more G0/G1 phase cells and less G2/M phase cells relative to the shNC+vector group; in contrast, the shNC+RelA group displayed more S and G2/M phase cells and less G0/G1 phase cells (p <0.01, Fig. 9D,F). Compared to shMIR155HG+RelA group, shNC+RelA group had less cells in the G0/G1 phase and more cells in the S phase and G2/M stage (p < 0.05, Fig. 9D,F), while shMIR155HG+vector group had more cells in the G0/G1 phase and less cells in G2/M stage (p < 0.001, Fig. 9D,F).

4. Discussion

This study revealed that BCSCs expressed MIR155HG at significant levels, which enhanced cell resistance to radiation and DNA damage repair while The Wnt signaling pathway is promoting stemness. crucial for cellular signal transduction, influencing cell growth, differentiation, and stem cell maintenance [22,23]. Normally, the Wnt pathway regulates cell fate decisions by modulating the stability and activity of β -catenin, excessive activation or mutations of which can enhance tumor cell stemness, thereby promoting tumor growth, metastasis, and drug resistance. KDM1A controls cancer cell stemness and facilitates thyroid cancer progress by means of the Wnt pathway [24]. BCSCs production and tumor growth are intimately associated with improper stimulation of the Wnt signaling system. Mortalin promotes epithelial-mesenchymal transition (EMT) and maintains BCSC stemness by activating the Wnt/GSK3 β/β -catenin signaling pathway [25]. Wnt signaling is improved by B4GalT5 to control BCSCs [26]. Herein, we identified

MIR155HG promotes the expression of β -catenin, suggesting that MIR155HG may promote BCSCs stemness and radioresistance via activating Wnt signaling pathway. Consequently, MIR155HG may function as a viable treatment target for radioresistant breast cancer.

By attaching to particular gene promoter regions, the transcription factor NF- κ B is essential for cell proliferation, proliferation, and survival [27]. According to gene expression profiling, triple-negative breast cancer can be regulated by the NF- κ B pathway [28]. Preclinical studies have shown that small molecule inhibitors of NF- κ B, such as aspirin and synthetic bromophosphates, demonstrate a strong anti-tumor response towards triple-negative breast cancer cells [29]. Additionally, NF- κ B is involved in regulating various tumor stem cells, including BCSCs. For example, Liu and Ma [30] found that inhibiting NF- κ B activity could delay the occurrence and growth of HER2positive breast cancer. A recent mechanistic study further revealed that NF- κ B can promote stem cell characteristics in breast cancer cells by regulating inflammatory cytokines through autocrine/paracrine pathways [31]. With bioinformatics analysis and experimental validation, we proved that MIR155HG may be transcriptionally activated by the NF- κB component RelA that binds to its promoter region. In line with existing reports, non-coding RNAs (ncRNAs) interact with NF- κ B. As a multifunctional transcription factor, NF- κ B is not only a target of many ncRNAs but also binds to the promoter regions of miRNAs to regulate their expressions. NF- κ B can mediate oxidative stress-induced apoptosis in myocardial cells by activating miR-21 expression [32]. In age-related inflammatory diseases such as osteoarthritis, NF- κ B can activate lncRNA Lethe expression to participate in disease progression [33]. Our cellular functional experiments showed that overexpression of the NF- κ B subunit *RelA* enhances radioresistance and stemness of BCSCs, which can be reversed by MIR155HG knockdown. Importantly, overexpression of NF- κ B subunit RelA promotes the expression of β -catenin, which is also reversed upon MIR155HG knockdown. Our results indicated that NF- κ B may activate Wnt signaling by upregulating MIR155HG, thereby reinforcing radioresistance and stemness in BCSCs. Herein, we observed potential differences in effects on different cell lines, MCF-7 and MDA-MB-231 that are human breast cancer cell lines with low and high metastatic potential, respectively. MDA-MB-231 is triple negative breast cancer cell lines, and MCF-7 cells have estrogen receptor positive, progesterone receptor positive and HER2 negative properties. These characteristics of the two cell lines may account for these differences in results. In addition, some genes are expressed differently in varied cells, which could contribute to the difference in results. But as speculations, additional research is warranted.

Of note, this study has some limitations. Despite using various experimental methods to validate our findings, further verification using *in vivo* models is necessary. Ad-

ditionally, we need to collect and validate the expression levels of MIR155HG and NF- κ B subunit RelA in clinical breast cancer samples to confirm the applicability of our findings in clinical practice. Our research demonstrated that NF- κ B/MIR155HG activates the Wnt pathway to induce radioresistance and stem-like characteristics in BCSCs, but there is a possibility that MIR155HG exerts effects by regulating other pathways other than the Wnt/ β -catenin pathway. In addition, how the level of NF- κ B entering the nucleus changes after transcription needs to be further investigated.

5. Conclusion

In summary, our findings indicate that NF- κ B activates MIR155HG to stimulate the Wnt signaling pathway, thus inducing radioresistance and stem-like characteristics in BCSCs. These discoveries highlight the significance of the NF- κ B-MIR155HG-Wnt signaling axis in therapeutic resistance and tumor progression of BCSCs, promoting further understanding of the molecular function of MIR155HG in BCSCs and supporting the development of novel therapeutic targets and strategies.

Availability of Data and Materials

The analyzed data sets generated during the study are available from the corresponding author on reasonable request.

Author Contributions

Substantial contributions to conception and design: YBX. Data acquisition, data analysis and interpretation: GML, LY, CZR. Drafting the article or critically revising it for important intellectual content: YBX. Final approval of the version to be published: All authors. Agreement to be accountable for all aspects of the work in ensuring that questions related to the accuracy or integrity of the work are appropriately investigated and resolved: All authors. All authors contributed to editorial changes in the manuscript.

Ethics Approval and Consent to Participate

Not applicable.

Acknowledgment

Not applicable.

Funding

This work was supported by the Zhejiang Province Medical Project [2020KY842].

Conflict of Interest

The authors declare no conflict of interest.



References

- [1] Sung H, Ferlay J, Siegel RL, Laversanne M, Soerjomataram I, Jemal A, *et al.* Global Cancer Statistics 2020: GLOBOCAN Estimates of Incidence and Mortality Worldwide for 36 Cancers in 185 Countries. CA: A Cancer Journal of Clinicians. 2021; 71: 209–249. https://doi.org/10.3322/caac.21660.
- [2] Obeagu EI, Obeagu GU. Breast cancer: A review of risk factors and diagnosis. Medicine. 2024; 103: e36905. https://doi.org/10. 1097/MD.0000000000036905.
- [3] Esteva FJ, Hubbard-Lucey VM, Tang J, Pusztai L. Immunotherapy and targeted therapy combinations in metastatic breast cancer. The Lancet. Oncology. 2019; 20: e175–e186. https://doi.org/10.1016/S1470-2045(19)30026-9.
- [4] Schulz A, Meyer F, Dubrovska A, Borgmann K. Cancer Stem Cells and Radioresistance: DNA Repair and Beyond. Cancers. 2019; 11: 862. https://doi.org/10.3390/cancers11060862.
- [5] Bao S, Wu Q, McLendon RE, Hao Y, Shi Q, Hjelmeland AB, et al. Glioma stem cells promote radioresistance by preferential activation of the DNA damage response. Nature. 2006; 444: 756–760. https://doi.org/10.1038/nature05236.
- [6] Zhang L, Chen W, Liu S, Chen C. Targeting Breast Cancer Stem Cells. International Journal of Biological Sciences. 2023; 19: 552–570. https://doi.org/10.7150/ijbs.76187.
- [7] Yang W, Huang XD, Zhang T, Zhou YB, Zou YC, Zhang J. LncRNA MIR155HG functions as a ceRNA of miR-223-3p to promote cell pyroptosis in human degenerative NP cells. Clinical and Experimental Immunology. 2022; 207: 241–252. https://doi.org/10.1093/cei/uxab030.
- [8] Rai KR, Liao Y, Cai M, Qiu H, Wen F, Peng M, et al. MIR155HG Plays a Bivalent Role in Regulating Innate Antiviral Immunity by Encoding Long Noncoding RNA-155 and microRNA-155-5p. mBio. 2022; 13: e0251022. https://doi.org/10.1128/mbio.02510-22.
- [9] Peng L, Chen Z, Chen Y, Wang X, Tang N. MIR155HG is a prognostic biomarker and associated with immune infiltration and immune checkpoint molecules expression in multiple cancers. Cancer Medicine. 2019; 8: 7161–7173. https://doi.org/10. 1002/cam4.2583.
- [10] Morman RE. BATF Regulation of Nfil3, Wnt10a, and miR155hg during Lymphocyte Activation Critical for T Cell Differentiation and Antibody Class Switch Recombination. European Journal of Immunology. 2018; 48:1492–1505.
- [11] Baytak E, Gong Q, Akman B, Yuan H, Chan WC, Küçük C. Whole transcriptome analysis reveals dysregulated oncogenic lncRNAs in natural killer/T-cell lymphoma and establishes MIR155HG as a target of PRDM1. Tumour Biology: the Journal of the International Society for Oncodevelopmental Biology and Medicine. 2017; 39: 1010428317701648. https://doi.org/10.1177/1010428317701648.
- [12] Shen L, Li Y, Hu G, Huang Y, Song X, Yu S, *et al.* MIR155HG Knockdown Inhibited the Progression of Cervical Cancer by Binding SRSF1. OncoTargets and Therapy. 2020; 13: 12043–12054. https://doi.org/10.2147/OTT.S267594.
- [13] Huo J, Wang Y, Zhang Y, Wang W, Yang P, Zhao W, et al. The LncRNA MIR155HG is Upregulated by SP1 in Melanoma Cells and Drives Melanoma Progression via Modulating the MiR-485-3p/PSIP1 Axis. Anti-cancer Agents in Medicinal Chemistry. 2022; 22: 152–159. https://doi.org/10.2174/1871520621666210322092906.
- [14] Yim RL, Wong KY, Kwong YL, Loong F, Leung CY, Chu R, et al. Methylation of miR-155-3p in mantle cell lymphoma and other non-Hodgkin's lymphomas. Oncotarget. 2014; 5: 9770–9782. https://doi.org/10.18632/oncotarget.2390.
- [15] Bao Z, Zhang N, Niu W, Mu M, Zhang X, Hu S, et al. Exosomal miR-155-5p derived from glioma stem-like cells promotes mesenchymal transition via targeting ACOT12. Cell

- Death & Disease. 2022; 13: 725. https://doi.org/10.1038/s41419-022-05097-w.
- [16] Wu X, Wang Y, Yu T, Nie E, Hu Q, Wu W, et al. Blocking MIR155HG/miR-155 axis inhibits mesenchymal transition in glioma. Neuro-oncology. 2017; 19: 1195–1205. https://doi.org/ 10.1093/neuonc/nox017.
- [17] Wu W, Yu T, Wu Y, Tian W, Zhang J, Wang Y. The miR155HG/miR-185/ANXA2 loop contributes to glioblastoma growth and progression. Journal of Experimental & Clinical Cancer Research: CR. 2019; 38: 133. https://doi.org/10.1186/ s13046-019-1132-0.
- [18] Liu H, Zheng W, Chen Q, Zhou Y, Pan Y, Zhang J, et al. lncRNA CASC19 Contributes to Radioresistance of Nasopharyngeal Carcinoma by Promoting Autophagy via AMPK-mTOR Pathway. International Journal of Molecular Sciences. 2021; 22: 1407. https://doi.org/10.3390/ijms22031407.
- [19] Yang Y, Zhou H, Zhang G, Xue X. Targeting the canonical Wnt/β-catenin pathway in cancer radioresistance: Updates on the molecular mechanisms. Journal of Cancer Research and Therapeutics. 2019; 15: 272–277. https://doi.org/10.4103/jcrt.J CRT 421 18.
- [20] Jang JY, Kim MK, Jeon YK, Joung YK, Park KD, Kim CW. Adenovirus adenine nucleotide translocator-2 shRNA effectively induces apoptosis and enhances chemosensitivity by the down-regulation of ABCG2 in breast cancer stem-like cells. Experimental & Molecular Medicine. 2012; 44: 251–259. https://doi.org/10.3858/emm.2012.44.4.019.
- [21] Liang Y, Zhou X, Xie Q, Sun H, Huang K, Chen H, et al. CD146 interaction with integrin β1 activates LATS1-YAP signaling and induces radiation-resistance in breast cancer cells. Cancer Letters. 2022; 546: 215856. https://doi.org/10.1016/j.canlet.2022. 215856.
- [22] Banerjee A, Jothimani G, Prasad SV, Marotta F, Pathak S. Targeting Wnt Signaling through Small molecules in Governing Stem Cell Fate and Diseases. Endocrine, Metabolic & Immune Disorders Drug Targets. 2019; 19: 233–246. https://doi.org/10.2174/1871530319666190118103907.
- [23] Katoh M, Katoh M. WNT signaling and cancer stemness. Essays in Biochemistry. 2022; 66: 319–331. https://doi.org/10.1042/EB C20220016.
- [24] Zhang W, Ruan X, Li Y, Zhi J, Hu L, Hou X, et al. KDM1A promotes thyroid cancer progression and maintains stemness through the Wnt/β-catenin signaling pathway. Theranostics. 2022; 12: 1500–1517. https://doi.org/10.7150/thno.66142.
- [25] Wei B, Cao J, Tian JH, Yu CY, Huang Q, Yu JJ, *et al.* Mortalin maintains breast cancer stem cells stemness via activation of Wnt/GSK3β/β-catenin signaling pathway. American Journal of Cancer Research. 2021; 11: 2696–2716.
- [26] Tang W, Li M, Qi X, Li J. β1,4-Galactosyltransferase V Modulates Breast Cancer Stem Cells through Wnt/β-catenin Signaling Pathway. Cancer Research and Treatment. 2020; 52: 1084–1102. https://doi.org/10.4143/crt.2020.093.
- [27] Carrà G, Lingua MF, Maffeo B, Taulli R, Morotti A. P53 vs NF-κB: the role of nuclear factor-kappa B in the regulation of p53 activity and vice versa. Cellular and Molecular Life Sciences: CMLS. 2020; 77: 4449–4458. https://doi.org/10.1007/ s00018-020-03524-9.
- [28] Espinoza-Sánchez NA, Győrffy B, Fuentes-Pananá EM, Götte M. Differential impact of classical and non-canonical NF-κB pathway-related gene expression on the survival of breast cancer patients. Journal of Cancer. 2019; 10: 5191–5211. https://doi.org/10.7150/jca.34302.
- [29] Poma P, Labbozzetta M, D'Alessandro N, Notarbartolo M. NFκB Is a Potential Molecular Drug Target in Triple-Negative Breast Cancers. Omics: a Journal of Integrative Biology. 2017; 21: 225–231. https://doi.org/10.1089/omi.2017.0020.
- [30] Liu J, Ma DWL. The role of n-3 polyunsaturated fatty acids in



- the prevention and treatment of breast cancer. Nutrients. 2014; 6: 5184–5223. https://doi.org/10.3390/nu6115184.
- [31] Huang CK, Yang CY, Jeng YM, Chen CL, Wu HH, Chang YC, et al. Autocrine/paracrine mechanism of interleukin-17B receptor promotes breast tumorigenesis through NF-κB-mediated antiapoptotic pathway. Oncogene. 2014; 33: 2968–2977. https://doi.org/10.1038/onc.2013.268.
- [32] Wei C, Li L, Kim IK, Sun P, Gupta S. NF- κ B mediated miR-21
- regulation in cardiomyocytes apoptosis under oxidative stress. Free Radical Research. 2014; 48: 282–291. https://doi.org/10.3109/10715762.2013.865839.
- [33] Feng T, Wu QF. A review of non-coding RNA related to NFκB signaling pathway in the pathogenesis of osteoarthritis. International Immunopharmacology. 2022; 106: 108607. https://doi.org/10.1016/j.intimp.2022.108607.

